

# Small-scale Sr isotope investigation of clinopyroxenes from peridotite xenoliths by laser ablation MC-ICP-MS—implications for mantle metasomatism

S.S. Schmidberger<sup>a,b,\*</sup>, A. Simonetti<sup>b</sup>, D. Francis<sup>a</sup>

<sup>a</sup>Earth and Planetary Sciences, McGill University, 3450 University Street, Montréal, Québec, Canada H3A 2A7

<sup>b</sup>GEOTOP, Université du Québec à Montréal, CP 8888 succ. Centreville, Montréal, Québec, Canada H3C 3P8

Received 1 February 2002; accepted 31 March 2003

## Abstract

Although numerous studies have shown that mantle xenoliths are isotopically heterogeneous on a hand specimen scale, experimental data imply that isotopic equilibrium should be attained within single mineral grains in the upper mantle. Until recently, this prediction has not been verified because of the difficulty of analyzing individual grains. We report in situ  $^{87}\text{Sr}/^{86}\text{Sr}$  compositions of clinopyroxenes in garnet peridotite xenoliths from the Nikos kimberlite, Somerset Island (Arctic Canada) obtained by laser ablation MC-ICP-MS. Results for five different peridotites indicate the existence of large Sr isotope variations within individual xenolith samples, varying from 0.5‰ to as much as 1.1‰ (3 to 8 parts in 7000). This study is the first to document isotopic heterogeneity in peridotite xenoliths at the scale of individual grains. Multiple analyses of the same grain, however, indicate intra-grain Sr isotopic equilibrium.

The Sr isotopic ratios for individual clinopyroxene grains correlate with major element abundances such as  $\text{SiO}_2$  and  $\text{TiO}_2$ , and trend towards the composition of the host Nikos kimberlite. It thus appears likely that the Sr isotope heterogeneities recorded by the clinopyroxenes are the result of metasomatic interaction with the host kimberlite magma. The preservation of Sr isotopic variability in clinopyroxene separates from different peridotite samples and between clinopyroxene grains of individual xenoliths suggests that metasomatism occurred just prior to or during kimberlite transport. The Sr isotope heterogeneities documented here for a single peridotite phase suggest that isotopic compositions obtained on mineral separates from peridotite xenoliths likely represent weighted averages and could be less homogenous than previously assumed.

© 2003 Elsevier Science B.V. All rights reserved.

*Keywords:* Clinopyroxene; Isotope heterogeneity; Laser ablation; Peridotite; Sr isotopes

## 1. Introduction

Radiogenic isotope data from mid-ocean ridge basalts (MORBs) and ocean island basalts (OIBs) indicate that the Earth's mantle is heterogeneous in isotopic composition (see Allègre et al., 1986; Zindler and Hart, 1986; Hart et al., 1992; Hofmann, 1997 and references therein). Similarly, Nd, Pb, Os and Sr iso-

\* Corresponding author. GEOTOP, Université du Québec à Montréal, CP 8888 succ. Centreville, Montréal, Québec, Canada H3C 3P8. Tel.: +1-514-987-3000x7019.

E-mail address: schmidberger.stefanie@courrier.uqam.ca (S.S. Schmidberger).

tope data for peridotite xenoliths hosted by kimberlites and alkali basalts indicate a large variation in isotope compositions for the subcontinental mantle (e.g. Menzies and Murthy, 1980; Kramers et al., 1983; Walker et al., 1989; Hawkesworth et al., 1990). This heterogeneity appears to be the result of multiple episodes of metasomatic activity (e.g. melt or fluid interaction), and has been documented in many peridotite xenolith suites from cratonic areas (e.g. Yaxley et al., 1991; Rudnick et al., 1993). U–Pb ages of metasomatized harzburgite (Kinny and Dawson, 1992) and the preservation of oxygen isotope disequilibrium amongst constituent peridotite minerals (Zhang et al., 2000) have been interpreted to indicate that the timing of mantle metasomatism and kimberlite emplacement may essentially be contemporaneous.

Hofmann and Hart (1978) have argued, on the basis of limited experimental diffusion data, that the mantle is heterogeneous on a regional scale, but homogeneous on the scale of individual grains. Sneering et al. (1984) subsequently reported that at near solidus temperatures, Sr diffusion in peridotite clinopyroxene is sufficiently rapid to easily maintain isotopic equilibrium between grains. Van Orman et al. (2001) have recently proposed that  $^{143}\text{Nd}/^{144}\text{Nd}$  isotopic equilibrium in clinopyroxene may be achieved in  $\sim 1$  Ma at near solidus conditions in peridotite (i.e.  $\sim 1450$  °C; 25 kb). However, the same experimental study also indicates that the time required for isotopic equilibration may increase to  $\sim 1000$  Ma at lower temperatures and pressures (i.e.  $\sim 1150$  °C; 15 kb) of the lithospheric mantle. Confirmation of the implications of these experimental results can only be accomplished by in situ isotopic investigations of mantle mineral(s) in peridotite.

Over the last decade, the introduction of multi-collector inductively coupled plasma mass spectrometry (MC-ICP-MS) instruments has provided the ability to accurately measure a large variety of stable and radiogenic isotope systems. This ability is attributable to the high ion transmission and flexibility of sample introduction in such instruments, the simultaneous detection of ion signals using analogue detectors and flat-top peaks. These features have combined to generate an instrument capable of performing isotope measurements with precisions comparable to those obtained by thermal ionization mass spectrom-

etry (TIMS). Moreover, the coupling of a laser ablation system to MC-ICP-MS instruments has added the potential of obtaining spatially resolved, high precision in situ measurements for a variety of radiogenic isotope systems, including  $^{87}\text{Sr}/^{86}\text{Sr}$  (Jackson et al., 2001 and references therein). Christensen et al. (1995) first reported the application of laser ablation MC-ICP-MS to Sr isotope studies, obtaining precise and accurate measurements on modern marine gastropods and plagioclase. These analytical data (long ablation times of 13–17 min) documented isotopic disequilibrium between two plagioclase grains from Long Valley basalts that has been interpreted as evidence of magma mixing. More recent laser ablation studies (ablation times of 30–60 s) have investigated the isotope zonation in single plagioclase (e.g. Davidson et al., 2001), and magmatic carbonate and apatite (Bizzarro et al., 2003).

Here we present in situ  $^{87}\text{Sr}/^{86}\text{Sr}$  analyses obtained by laser ablation MC-ICP-MS on clinopyroxene grains in peridotite xenoliths from the Nikos kimberlite, Somerset Island (Arctic Canada). These results are compared to those obtained by TIMS and solution mode MC-ICP-MS, which both represent weighted average values for a much larger population of clinopyroxene grains from the same rocks. The data document Sr isotopic variability between clinopyroxene grains within the same mantle xenolith, and provide information on the possible interaction with the host rock during kimberlite magmatism. Previous studies using bulk mineral separates have documented isotopic disequilibrium between different mineral phases in peridotite (McDonough and McCulloch, 1987) and clinopyroxene phenocrysts in alkaline magmas (Simionetti and Bell, 1993). To our knowledge, this is the first study to document small-scale Sr isotope variations in individual clinopyroxene grains that have equilibrated at great depths ( $>100$  km) in the Earth's mantle.

### 1.1. Somerset mantle xenoliths

The mantle xenoliths of this study were collected from the Nikos kimberlite, which was emplaced into the Archean crystalline basement and Paleozoic cover sequences of Somerset Island on the northern Canadian craton ( $73^{\circ}28'\text{N}$  and  $90^{\circ}58'\text{W}$ ; Frisch and Hunt, 1993; Pell, 1993). Magmatism occurred between 90 and 105 Ma ago, as indicated by U–Pb dates for

perovskites from Somerset Island kimberlites (Heaman, 1989; Smith et al., 1989) and a Rb–Sr whole-rock isochron obtained for the Nikos kimberlite ( $97 \pm 17$  Ma, MSWD = 1.1; Schmidberger et al., 2001). The Nikos mantle xenolith suite is dominated by well-preserved garnet peridotites that contain large crystals (1–10 mm) of olivine, orthopyroxene, clinopyroxene and garnet. Trace amounts (<1%) of phlogopite are present in a small number of peridotites, but amphibole is absent. Estimates of the temperature and pressure of last equilibration (800–1400 °C, 25–60 kb) indicate that the Nikos peridotites were sampled from depths of 80 to 190 km by their host kimberlite (Schmidberger and Francis, 1999). The high magnesium numbers (mg number =  $Mg/(Mg + Fe) = 0.90–0.93$ ) and olivine-rich mineralogy (avg. 80 wt.%) of the peridotites reflect their refractory nature and suggest that these xenoliths are the residues of large degrees of partial melting (Schmidberger and Francis, 1999; Schmidberger and Francis, 2001). In contrast to their depleted major element chemistry, however, the peridotite xenoliths are enriched in highly incompatible trace elements (e.g. large ion lithophile elements, LILE; light rare earth elements, LREE) relative to estimates for primitive mantle and chondrites (McDonough and Sun, 1995) as the result of metasomatism (Schmidberger and Francis, 2001). A detailed description of the mineralogy and major and trace element compositions of these mantle xenoliths can be found in Schmidberger and Francis (1999) and Schmidberger and Francis (2001).

### 1.2. Clinopyroxene

The emerald green clinopyroxenes of the Nikos peridotites are chromian diopsides (Schmidberger and Francis, 1999). The incompatible trace element compositions of clinopyroxene correlate with temperature and depth estimates of last equilibration and suggest that the peridotites can be divided into low-temperature (<1100 °C; 80–150 km) and high-temperature xenoliths (>1100 °C; 160–190 km). The clinopyroxenes of the low-temperature peridotites are characterized by high Sr (100–400 ppm) and LREE (e.g. Ce = 20–50 ppm) abundances compared to the clinopyroxenes of the high-temperature peridotites (Sr = 50–100 ppm; Ce = 2–8 ppm; Schmidberger and Francis, 2001). The present study is restricted to

clinopyroxene in the low-temperature peridotites because their significantly higher Sr contents facilitated in situ analysis.

The  $^{87}\text{Sr}/^{86}\text{Sr}$  values (0.7038–0.7046) obtained by TIMS for clinopyroxene separates from the low-temperature peridotites are significantly less radiogenic than their corresponding whole rock compositions ( $^{87}\text{Sr}/^{86}\text{Sr}_{(0.1\text{Ga})} = 0.7054–0.7066$ ). The Sr isotopic signatures of these clinopyroxenes indicate derivation from a time-integrated depleted mantle (Schmidberger et al., 2001).  $^{143}\text{Nd}/^{144}\text{Nd}_{(0.1\text{Ga})}$  ratios (0.51256–0.51268) obtained by TIMS on these clinopyroxene separates show little variation and are depleted relative to a chondrite reservoir at the time of kimberlite magmatism.

## 2. Analytical methods

Inclusion-free clinopyroxene grains were hand-picked from the low-temperature peridotites for laser ablation analyses and then washed in an ultrasonic bath with acetone, ultrapure water and 2.5 N HCl. The grains were subsequently embedded into epoxy mounts (25 mm diameter) and surfaces were polished to 0.3  $\mu\text{m}$ . In most cases, only one analysis per grain was possible, but two separate analyses were obtained on grains larger than 0.5 mm (see Table 1; Fig. 1).

In situ Sr isotope analyses were determined on a Micromass IsoProbe MC-ICP-MS coupled to a 193 nm (ArF) excimer laser (Compex 102; Lambda Physik) at GEOTOP, Université du Québec à Montréal. Table 2 lists the analytical parameters used in laser ablation experiments. Helium was used to flush-out the ablation cell instead of Ar since previous studies have clearly shown that the former increases instrument sensitivity due to a higher sample transport efficiency, and reduced deposition at the ablation site (e.g. Eggins et al., 1998; Horn et al., 2000; Fig. 1). Ar gas was mixed into the ‘sample-out’ line from the ablation cell prior to arrival at the plasma via a ‘y-connection’ to an ARIDUS<sup>®</sup> microconcentric nebulizer. Sr isotope data were obtained in static, multi-collection mode using six Faraday collectors. For each analysis, data acquisition consisted of a 50-s measurement of the gas blank prior to the start of ablation, similar to the method of Davidson et al. (2001) for an

Table 1  
Sr isotopic data determined by laser ablation and solution mode MC-ICP-MS

Sample	Grain No.	$^{87}\text{Sr}/^{86}\text{Sr}$	$^{84}\text{Sr}/^{86}\text{Sr}$	$^{84}\text{Sr}/^{88}\text{Sr}$	$^{88}\text{Sr}$ intensity (volts)	$^{85}\text{Rb}$ intensity (volts)	Rb/Sr	
NK1-2	1-1	0.70395 ± 5	0.0562 ± 2	0.00671 ± 2	4.08	0.00040	0.00012	
	1-2	0.70401 ± 4	0.0557 ± 2	0.00665 ± 2	4.11	0.00080	0.00023	
	2	0.70379 ± 7	0.0565 ± 2	0.00675 ± 3	2.26	0.00010	0.00004	
	3	0.70357 ± 5	0.0569 ± 2	0.00679 ± 2	2.86	0.00002	0.000007	
	4	0.70377 ± 6	0.0561 ± 2	0.00670 ± 2	2.93	0	0	
	5-1	0.70395 ± 5	0.0561 ± 2	0.00669 ± 2	3.41	0.00030	0.00010	
	5-2	0.70380 ± 5	0.0563 ± 2	0.00673 ± 3	3.38	0.00004	0.00002	
	6-1	0.70398 ± 7	0.0564 ± 2	0.00673 ± 2	3.24	0.00160	0.00058	
	6-2	0.70412 ± 3	0.0558 ± 2	0.00667 ± 2	3.74	0.00210	0.00065	
	7	0.70380 ± 5	0.0563 ± 2	0.00673 ± 3	3.12	0	0	
	8	0.70390 ± 4	0.0563 ± 2	0.00672 ± 3	3.31	0.00050	0.00018	
	Average	0.70388	0.0562 ± 6	0.00671 ± 10	3.31	0.00050	0.00017	
	Sol'n mode	0.70394 ± 2	0.05641 ± 3	0.006736 ± 4	4.21	0.00004		
	NK1-3	9	0.70416 ± 5	0.0560 ± 2	0.00669 ± 2	2.83	0.0008	0.00030
		10-1	0.70434 ± 5	0.0568 ± 2	0.00678 ± 2	2.79	0.0001	0.00004
		10-2	0.70431 ± 4	0.0574 ± 2	0.00685 ± 2	2.79	0.0002	0.00009
		11	0.70433 ± 4	0.0569 ± 2	0.00679 ± 3	4.11	0.0002	0.00006
		12	0.70454 ± 4	0.0563 ± 2	0.00672 ± 2	3.28	0.0014	0.00049
		13	0.70440 ± 4	0.0563 ± 2	0.00672 ± 2	3.44	0.0008	0.00026
14-1		0.70427 ± 5	0.0570 ± 2	0.00681 ± 2	3.48	0.0006	0.00020	
14-2		0.70444 ± 6	0.0569 ± 2	0.00680 ± 3	3.33	0.0011	0.00039	
15		0.70433 ± 4	0.0564 ± 2	0.00674 ± 2	3.21	0	0	
16		0.70447 ± 5	0.0560 ± 2	0.00669 ± 2	3.16	0	0	
17		0.70440 ± 6	0.0562 ± 2	0.00671 ± 3	3.47	0.0002	0.00005	
18		0.70457 ± 4	0.0569 ± 2	0.00679 ± 3	2.95	0.0004	0.00010	
19		0.70450 ± 5	0.0567 ± 2	0.00677 ± 3	3.24	0.0010	0.00035	
Average		0.70439	0.0566 ± 8	0.00676 ± 10	3.24	0.0005	0.00018	
TIMS		0.70415 ± 1	0.05653 ± 1	0.006750 ± 1	3.40	–		
Sol'n mode		0.70425 ± 2	0.05720 ± 2	0.006830 ± 2	5.13	0.0011		
NK1-4		20	0.70382 ± 6	0.0570 ± 2	0.00680 ± 2	3.22	0	0
		21-1	0.70395 ± 4	0.0568 ± 1	0.00678 ± 2	3.09	0.0003	0.00010
		21-2	0.70397 ± 9	0.0566 ± 3	0.00676 ± 4	3.04	0.0013	0.00048
	22	0.70404 ± 5	0.0570 ± 2	0.00680 ± 2	3.11	0.0006	0.00021	
	23-1	0.70392 ± 5	0.0568 ± 1	0.00679 ± 2	2.92	0.0002	0.00010	
	23-2	0.70395 ± 7	0.0566 ± 2	0.00676 ± 2	3.01	0.0006	0.00022	
	24	0.70402 ± 5	0.0561 ± 1	0.00670 ± 2	2.81	0.0006	0.00026	
	25	0.70382 ± 6	0.0558 ± 2	0.00667 ± 2	2.59	0.0001	0.00006	
	26	0.70380 ± 5	0.0566 ± 2	0.00676 ± 2	2.93	0.00001	0.000004	
	27	0.70390 ± 5	0.0564 ± 1	0.00673 ± 2	2.87	0.0006	0.00023	
	28	0.70387 ± 7	0.0563 ± 2	0.00672 ± 2	2.76	0.0006	0.00026	
	29	0.70400 ± 5	0.0561 ± 2	0.00670 ± 2	3.00	0.0001	0.00003	
	30	0.70372 ± 7	0.0567 ± 2	0.00677 ± 2	2.79	0.0002	0.00007	
	Average	0.70391	0.0565 ± 7	0.00675 ± 8	2.93	0.0004	0.00015	
	TIMS	0.70382 ± 1	0.05652 ± 1	0.006751 ± 1	3.80	–		
	Sol'n mode	0.70404 ± 2	0.05674 ± 3	0.006775 ± 4	4.53	0.00009		
	NK2-3	31	0.70474 ± 5	0.0564 ± 5	0.00674 ± 5	2.73	0.00070	0.00030
		32	0.70442 ± 6	0.0569 ± 3	0.00679 ± 4	3.78	0.00004	0.00001
		33	0.70521 ± 10	0.0564 ± 2	0.00673 ± 2	2.54	0.00190	0.00240
34		0.70489 ± 6	0.0559 ± 3	0.00668 ± 3	1.58	0.00003	0.00086	
35		0.70485 ± 5	0.0566 ± 2	0.00676 ± 3	2.33	0.00080	0.00039	
36-1		0.70495 ± 7	0.0566 ± 3	0.00676 ± 3	2.09	0.00070	0.00037	
36-2		0.70508 ± 7	0.0571 ± 1	0.00682 ± 2	3.26	0.00380	0.00132	

Table 1 (continued)

Sample	Grain No.	$^{87}\text{Sr}/^{86}\text{Sr}$	$^{84}\text{Sr}/^{86}\text{Sr}$	$^{84}\text{Sr}/^{88}\text{Sr}$	$^{88}\text{Sr}$ intensity (volts)	$^{85}\text{Rb}$ intensity (volts)	Rb/Sr
NK2-3	37	0.70485 ± 4	0.0566 ± 2	0.00675 ± 2	3.12	0.00190	0.00070
	38	0.70465 ± 5	0.0568 ± 1	0.00678 ± 2	3.40	0.00180	0.00062
	Average	0.70485	0.0566 ± 6	0.00676 ± 1	2.76	0.0013	0.00051
	TIMS	0.70458 ± 1	0.05652 ± 1	0.006748 ± 1	2.00	–	
	Sol'n mode	0.70434 ± 1	0.05694 ± 3	0.006798 ± 3	5.91	0.0001	
NK2-10	39-1	0.70436 ± 5	0.0560 ± 2	0.00669 ± 3	3.57	0	0
	39-2	0.70427 ± 5	0.0561 ± 2	0.00670 ± 2	3.52	0.00003	0.00001
	40	0.70485 ± 7	0.0560 ± 3	0.00669 ± 3	2.47	0.00170	0.00078
	41	0.70461 ± 4	0.0561 ± 1	0.00670 ± 1	3.01	0.00110	0.00042
	42	0.70447 ± 10	0.0563 ± 1	0.00673 ± 1	2.57	0.00100	0.00043
	43-1	0.70447 ± 4	0.0568 ± 1	0.00678 ± 1	3.00	0.00060	0.00024
	43-2	0.70438 ± 4	0.0569 ± 1	0.00679 ± 1	3.00	0.00040	0.00016
	44	0.70451 ± 6	0.0566 ± 1	0.00676 ± 2	3.01	0.00140	0.00052
	45	0.70432 ± 5	0.0564 ± 3	0.00673 ± 3	2.78	0	0
	46	0.70450 ± 6	0.0568 ± 2	0.00678 ± 2	2.85	0.00100	0.00041
	Average	0.70449	0.0565 ± 6	0.00674 ± 10	3.02	0.0016	0.00030
	Sol'n mode	0.70449 ± 2	0.05692 ± 8	0.006796 ± 9	4.50	0.0030	
	NBS 987 100ppb	Sol'n mode n=5	0.71025 ± 7	0.05659 ± 29	0.006758 ± 34		

IsoProbe MC-ICP-MS. This measurement is critical since it monitors  $^{86}\text{Kr}$ , which interferes with the  $^{86}\text{Sr}$  signal. Measured isotope ratios were corrected for instrument fractionation using the exponential law (Russell et al., 1978) and a  $^{86}\text{Sr}/^{88}\text{Sr}$  value of 0.1194 (see Faure, 1986). The isobaric interference of  $^{87}\text{Rb}$  was monitored and corrected for using the  $^{85}\text{Rb}$  ion signal (Table 1). Davidson et al. (2001) investigated the relationship between the Rb/Sr ratio in feldspars and their measured  $^{87}\text{Sr}/^{86}\text{Sr}$  value

obtained during laser ablation using Rb-doped synthetic glass standards. The results indicated that for standards with Rb/Sr ratios of  $\sim 0.0015$ , the  $^{87}\text{Sr}/^{86}\text{Sr}$  values obtained by laser ablation were roughly 0.0001 higher than those obtained by TIMS analysis on the same standards. The Rb/Sr values for the clinopyroxenes investigated here (with the exception of one grain), however, are much lower than 0.0015 (Table 1 and Schmidberger et al., 2001) and, therefore, the  $^{87}\text{Rb}$  interference on the measured  $^{87}\text{Sr}/^{86}\text{Sr}$  is considered negligible. In the extreme case, this interference is approximately the same magnitude as the  $2\sigma$  internal precision ( $< 0.0001$ ) associated with the  $^{87}\text{Sr}/^{86}\text{Sr}$  value for individual laser ablation analyses. The effectiveness of the interference correction for Kr applied to the analyses can be directly evaluated by monitoring the invariant  $^{84}\text{Sr}/^{86}\text{Sr}$  and  $^{84}\text{Sr}/^{88}\text{Sr}$  ratios (Table 1), and compar-

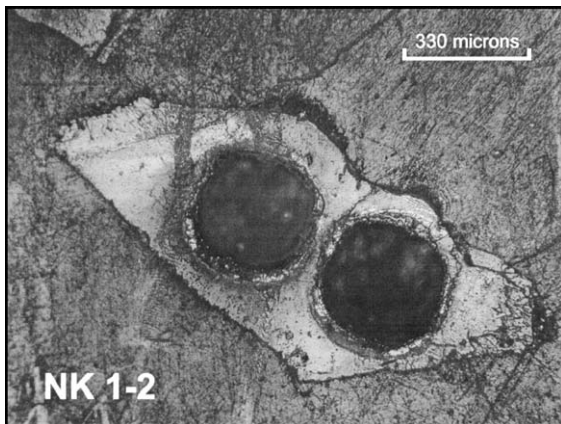


Fig. 1. Microphotograph of two laser ablation pits (330  $\mu\text{m}$ ) within a single clinopyroxene grain for sample NK1-2.

Table 2

Analytical parameters used in laser ablation experiments

He flow into ablation cell	0.6 l/min
Laser pulse energy	190 to 200 mJ
Laser pulse duration	25 ns
Repetition rate	15 Hz
Energy density	7 J/cm <sup>2</sup>
Spot size	330 $\mu\text{m}$

ing these to their accepted reference values (0.0565 and 0.00675; respectively).

Hydrogen acts as reactive gas in collision (and reaction) cells such as that of the IsoProbe instrument, and is effective in eliminating certain isobaric interferences (e.g. Mason, 2001). Hydrogen gas was mixed with Ar at a ratio of 1:20 in the hexapole housing. In this study, hydrogen proved effective in eliminating potential isobaric interferences related to the production of Fe-oxides (atomic masses  $86 = {}^{54}\text{Fe} + {}^{32}\text{O}$  and  $88 = {}^{56}\text{Fe} + {}^{32}\text{O}$ ) in Fe-bearing matrices such as the clinopyroxenes of this study (2.0 to 2.4 wt.% FeO; Schmidberger and Francis, 2001). This is supported by the fact that no correlations exist between FeO contents in the clinopyroxenes and their respective Sr isotopic ratios (see also Discussion and Tables 1 and 3).

Ion beam intensities for most samples varied from  $\sim 3$  to  $4 \times 10^{-11}$  A of  ${}^{88}\text{Sr}$ . Subsequent to the start of laser ablation, two half mass-unit baseline measurements were obtained for each Faraday collector (within the mass range 82.5 to 88.5), followed by ion signal measurements of 100-s intervals (50 integrations of 2 s each). Time-resolved analysis for the ablation runs was not needed because of the simultaneous acquisition of the ion signals (multi-collection), and the relative stability of the ion signals (e.g. average error  $\sim 0.6\%$  for  ${}^{88}\text{Sr}$ ) resulting in high in run precision (Table 1).

Sr isotopic analysis in solution mode MC-ICP-MS and TIMS was performed on  $\sim 0.030$  and  $0.100$  g (i.e. 50 and 150 grains) of clinopyroxene separate, respectively, which were dissolved at  $140^\circ\text{C}$  in Savillex<sup>®</sup> vials. Sr was separated using conventional chromatographic techniques, and typical procedural blanks were  $< 70$  pg. TIMS analyses (Schmidberger et al., 2001) were obtained using a VG Sector54 mass spectrometer operated in the static multicollection mode. Sr aliquots were loaded using a TaF solution on single W filaments. Samples for solution mode analysis on the MC-ICP-MS were aspirated into the ICP source using an Aridus<sup>®</sup> microconcentric nebulizer at an uptake rate of approximately 50  $\mu\text{l}/\text{min}$  (verified periodically). The parameters for data acquisition in solution mode are similar to those used during laser ablation (described above) except that an integration time of 10 s/cycle was used for a block of 50 scans.

### 2.1. In-house standard

The Sr isotopic composition of a sample of modern-day coral ( $\sim 3500$  years old; U–Th age, B. Ghaleb, personal communication) from the southwestern Pacific Ocean was investigated in order to determine the external reproducibility ( $2\sigma$ ) of the laser ablation work employed in this study. The laser ablation experiments were conducted over 4 days, and repeated measurements ( $n=40$ ; 80- $\mu\text{m}$  spot size) yielded an average  ${}^{87}\text{Sr}/{}^{86}\text{Sr}$  value of  $0.70910 \pm 0.00005$  ( $2\sigma$  standard deviation; extension of the work published in Bizzarro et al., 2003) with corresponding average  ${}^{84}\text{Sr}/{}^{86}\text{Sr}$  and  ${}^{84}\text{Sr}/{}^{88}\text{Sr}$  ratios of  $0.0563 \pm 0.0004$  and  $0.00672 \pm 0.00005$  ( $2\sigma$  standard deviation), respectively (Fig. 2a). TIMS measurements were obtained on four separate fragments of the coral to investigate the accuracy of the laser ablation results. The fragments (0.05 g each) were dissolved, and processed through conventional cation exchange chromatography. The Sr isotopic results obtained by TIMS yield an average  ${}^{87}\text{Sr}/{}^{86}\text{Sr}$  value of  $0.709098 \pm 0.000019$  ( $2\sigma$  standard deviation; Bizzarro et al., 2003), which is identical to the average Sr isotopic composition obtained in the laser ablation analyses. This provides strong evidence for the accuracy of the laser ablation results obtained here.

The Sr isotopic composition of a mollusk sample from a terrace deposit located at Esmeraldas (northwestern Ecuador) yielding a U–Th date of  $\sim 55000$  years was also investigated for comparison. The stratigraphic age for the surrounding terrace deposit, however, is  $\sim 125000$  years (B. Ghaleb, personal communication), a discrepancy that has been attributed to post-depositional alteration of the mollusk. Fig. 2b illustrates the measured  ${}^{87}\text{Sr}/{}^{86}\text{Sr}$  values obtained for 30 analyses of the mollusk over the period of this study. The average  ${}^{87}\text{Sr}/{}^{86}\text{Sr}$  value is  $0.70901 \pm 0.0001$  ( $2\sigma$  standard deviation), and the average  ${}^{84}\text{Sr}/{}^{86}\text{Sr}$  and  ${}^{84}\text{Sr}/{}^{88}\text{Sr}$  ratios obtained are  $0.0567 \pm 0.0004$  ( $2\sigma$ ) and  $0.00677 \pm 0.00008$  ( $2\sigma$ ), respectively. In contrast to the laser ablation results obtained from the coral, the external reproducibility ( $2\sigma$ ,  $\pm 0.0001$ ) for the Sr isotopic measurements of the mollusk is twice as large, and roughly double the average internal precision for the individual ablation analyses (Fig. 2b). Thus, the large-scale isotopic homogeneity of the mollusk was investigated using

Table 3  
Major element compositions for clinopyroxenes determined using electron microprobe analysis

Sample	Grain No.	SiO <sub>2</sub>	TiO <sub>2</sub>	Al <sub>2</sub> O <sub>3</sub>	FeO	MnO	MgO	CaO	Na <sub>2</sub> O	K <sub>2</sub> O	Cr <sub>2</sub> O <sub>3</sub>	NiO	Total	Mg#
NK1-2	1	53.99	0.13	2.72	2.27	0.07	16.09	19.62	2.26	0.01	2.31	0.03	99.51	0.927
	2	54.25	0.11	2.71	2.27	0.07	16.03	19.53	2.26	0.01	2.32	0.04	99.61	0.926
	3	54.15	0.11	2.71	2.30	0.08	16.17	19.56	2.25	0.01	2.29	0.04	99.67	0.926
	4	54.19	0.12	2.73	2.28	0.06	16.02	19.41	2.28	0.01	2.38	0.04	99.52	0.926
	5	54.17	0.12	2.66	2.27	0.07	16.11	19.44	2.29	0.01	2.29	0.03	99.48	0.927
	6	54.18	0.12	2.66	2.21	0.07	16.10	19.75	2.22	0.01	2.25	0.02	99.59	0.928
	7	54.04	0.12	2.70	2.25	0.07	16.08	19.61	2.24	0.01	2.27	0.03	99.42	0.927
	8	54.06	0.12	2.73	2.34	0.07	16.18	19.71	2.23	0.02	2.05	0.04	99.55	0.925
NK1-3	9	54.48	0.13	2.98	2.37	0.08	15.77	19.09	2.51	0.01	2.17	0.03	99.61	0.922
	10	54.52	0.13	3.08	2.37	0.07	15.92	19.02	2.56	0.02	2.18	0.03	99.88	0.923
	11	54.19	0.14	3.06	2.36	0.08	15.73	19.00	2.54	0.01	2.17	0.03	99.31	0.922
	12	54.40	0.13	3.23	2.39	0.07	15.81	18.87	2.55	0.01	2.05	0.03	99.55	0.922
	13	54.19	0.14	3.20	2.36	0.07	15.80	18.83	2.59	0.01	2.09	0.03	99.32	0.923
	14	54.18	0.14	3.23	2.36	0.07	15.66	18.83	2.60	0.02	2.24	0.03	99.36	0.922
	15	54.19	0.11	2.73	2.34	0.07	15.88	19.18	2.37	0.02	2.15	0.03	99.06	0.924
	16	54.17	0.14	3.16	2.39	0.07	15.69	18.78	2.54	0.01	2.14	0.03	99.11	0.921
	17	54.10	0.15	3.34	2.35	0.07	15.59	18.71	2.72	0.02	2.34	0.04	99.44	0.922
	18	54.08	0.13	2.96	2.38	0.08	15.87	18.93	2.49	0.01	2.19	0.03	99.15	0.922
NK1-4	19	54.31	0.14	3.18	2.34	0.07	15.81	18.82	2.59	0.01	2.26	0.03	99.57	0.923
	20	54.51	0.12	2.73	2.30	0.07	16.10	19.72	2.29	0.01	2.23	0.03	100.11	0.926
	21	54.30	0.12	2.70	2.32	0.07	16.24	19.76	2.23	0.01	2.14	0.03	99.94	0.926
	22	54.17	0.14	2.73	2.30	0.06	16.11	19.68	2.22	0.01	2.13	0.05	99.60	0.926
	24	54.33	0.13	2.75	2.32	0.07	16.16	19.50	2.26	0.01	2.23	0.04	99.81	0.926
	25	54.12	0.12	2.73	2.28	0.06	16.09	19.69	2.27	0.01	2.26	0.03	99.67	0.926
	26	54.21	0.12	2.73	2.31	0.06	16.16	19.56	2.30	0.01	2.33	0.04	99.83	0.926
	27	54.11	0.11	2.73	2.32	0.07	16.26	19.69	2.24	0.01	2.10	0.02	99.67	0.926
	28	54.44	0.13	2.75	2.32	0.07	16.18	19.66	2.26	0.01	2.25	0.03	100.10	0.925
	29	54.11	0.12	2.73	2.33	0.07	16.37	19.58	2.19	0.01	2.02	0.03	99.56	0.926
	30	54.20	0.14	2.73	2.31	0.09	16.25	19.42	2.26	0.02	2.30	0.09	99.81	0.926
	NK2-3	31	53.77	0.18	2.56	2.03	0.06	16.15	21.07	1.79	0.01	1.73	0.02	99.37
32		53.85	0.19	2.60	2.06	0.06	16.11	20.99	1.80	0.01	1.77	0.03	99.46	0.933
33		53.82	0.16	2.50	2.06	0.06	16.19	21.07	1.78	0.01	1.72	0.03	99.38	0.933
34		54.06	0.18	2.57	2.08	0.06	16.21	20.98	1.76	0.01	1.67	0.03	99.61	0.933
35		53.69	0.21	3.03	2.03	0.06	15.82	20.56	2.07	0.01	1.90	0.03	99.41	0.933
36		53.63	0.20	3.05	2.04	0.06	15.81	20.53	2.03	0.02	1.89	0.03	99.29	0.932
37		53.63	0.21	3.07	1.99	0.06	15.76	20.55	2.05	0.01	1.86	0.03	99.21	0.934
38		53.82	0.21	2.81	2.05	0.06	15.98	20.87	1.93	0.01	1.87	0.03	99.63	0.933
NK2-10	39	54.24	0.15	2.97	2.36	0.07	15.91	19.12	2.40	0.02	2.17	0.04	99.45	0.923
	40	53.91	0.16	2.90	2.37	0.07	15.89	19.18	2.39	0.01	2.35	0.04	99.27	0.923
	41	54.05	0.15	2.89	2.36	0.07	15.87	18.99	2.42	0.01	2.39	0.03	99.23	0.923
	42	54.15	0.15	2.89	2.36	0.07	15.89	19.09	2.40	0.01	2.36	0.07	99.43	0.923
	43	54.25	0.16	2.89	2.35	0.07	15.92	19.30	2.38	0.01	2.26	0.02	99.62	0.923
	44	54.24	0.15	2.88	2.36	0.07	15.99	19.26	2.35	0.01	2.20	0.03	99.55	0.924
	45	54.14	0.15	2.89	2.35	0.06	15.91	19.14	2.44	0.02	2.36	0.05	99.52	0.923
	46	54.13	0.14	2.91	2.35	0.07	15.90	19.12	2.38	0.02	2.35	0.03	99.40	0.923

Procedures for electron microprobe analysis are described in Schmidberger and Francis (1999).

two sample fragments (0.050 and 0.130 g) taken randomly from the complementary piece of the one used for the laser ablation experiment. These were dissolved, then processed through conventional cat-

ion exchange chromatography, and analyzed in solution mode MC-ICP-MS. The <sup>87</sup>Sr/<sup>86</sup>Sr values for the two fragments (0.70896 and 0.70912; Fig. 2) indicate some isotopic heterogeneity (difference of ~0.00015),

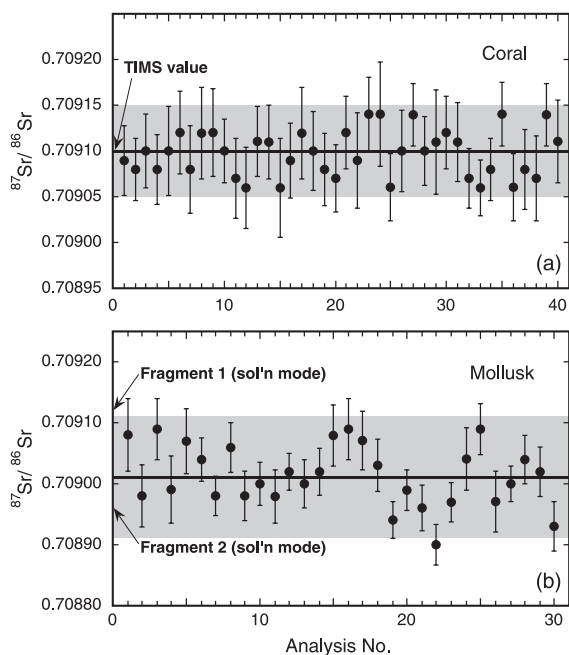


Fig. 2. Individual  $^{87}\text{Sr}/^{86}\text{Sr}$  isotope analyses of the 'in-house' (a) coral and (b) mollusk standards using laser ablation MC-ICP-MS. The Sr isotopic compositions for the coral standard determined by TIMS analysis and for two separate fragments of the mollusk standard determined by solution mode MC-ICP-MS are shown for comparison. Shaded array outlines the calculated ( $2\sigma$ ) external reproducibility in both diagrams ( $\pm 0.00005$  for the coral;  $\pm 0.0001$  for the mollusk). Error bars represent internal precisions of individual laser ablation analyses at the  $2\sigma$  level. (Analysis nos. 31 to 40 for the coral have been added to the results from Bizzarro et al., 2003).

but essentially bracket the individual laser ablation analyses. Thus, the Sr isotopic variation observed in the laser ablation data for the mollusk is not entirely instrument-induced, but reflects the inherent isotopic heterogeneity of the sample. The combined laser ablation Sr isotopic ratios for coral and mollusk samples show the effectiveness of the methodology in detecting isotopic heterogeneity at the millimeter scale within a single sample.

The values obtained for the  $^{84}\text{Sr}/^{86}\text{Sr}$  and  $^{84}\text{Sr}/^{88}\text{Sr}$  measurements for both the coral and mollusk samples are within error of their accepted reference values (0.0565 and 0.00675, respectively), thus validating the technique and proving the effectiveness of the correction for the gas blank (i.e.  $^{86}\text{Kr}$ ). The average Sr isotopic ratio obtained for repeated anal-

yses ( $n=5$ ) of a 100-ppb solution of Sr standard NBS 987 on the days in which both solution mode and laser ablation analyses were carried out is listed in Table 1. These are identical to the accepted Sr isotopic values for this standard, thus supporting the validity of the isotope ratios for the clinopyroxene separates and mollusk fragments obtained in solution mode.

### 3. Results

Laser ablation MC-ICP-MS analyses were obtained on 46 grains of clinopyroxene from five low-temperature Nikos peridotites (total of 56 analyses; Table 1; Fig. 3). The results indicate a large variation in the  $^{87}\text{Sr}/^{86}\text{Sr}$  values within individual samples, with differences ranging from 0.0003 (0.5‰, NK1-4) to 0.0008 (1.1‰, NK2-3; Fig. 3). These intra-sample variations are much larger than the average  $2\sigma$  internal precision of individual laser analyses (Table 1), and the estimated external reproducibility of 0.00005 for the method. The fractionation-corrected  $^{84}\text{Sr}/^{86}\text{Sr}$  and  $^{84}\text{Sr}/^{88}\text{Sr}$  ratios define a restricted range, and the calculated average values are within error of the accepted reference values for the isotopic composition of natural Sr (0.0565 and 0.00675, respectively; Table 1). This provides an important check on the laser ablation results. Moreover, the laser ablation  $^{87}\text{Sr}/^{86}\text{Sr}$  values do not correlate with  $^{85}\text{Rb}$  intensities. These results suggest that the observed variation in  $^{87}\text{Sr}/^{86}\text{Sr}$  is an inherent feature of the clinopyroxene grains and not an analytical artefact.

The difference between the average  $^{87}\text{Sr}/^{86}\text{Sr}$  value calculated for individual laser ablation runs and the corresponding value obtained either by solution mode MC-ICP-MS or TIMS is  $\leq 0.0002$  (Table 1), with the exception of one sample (NK2-3), which will be discussed later. This result is remarkable given that solution mode MC-ICP-MS and TIMS Sr isotope analyses represent a much larger population of clinopyroxene grains ( $\sim 50$  and 150, respectively). The range in  $^{87}\text{Sr}/^{86}\text{Sr}$  compositions obtained by laser ablation for each sample, however, extends to both higher and lower values than those obtained by either TIMS or solution mode MC-ICP-MS (except for sample NK2-3; Table 1). These results are consistent with an interpretation that the  $^{87}\text{Sr}/^{86}\text{Sr}$  values obtained by

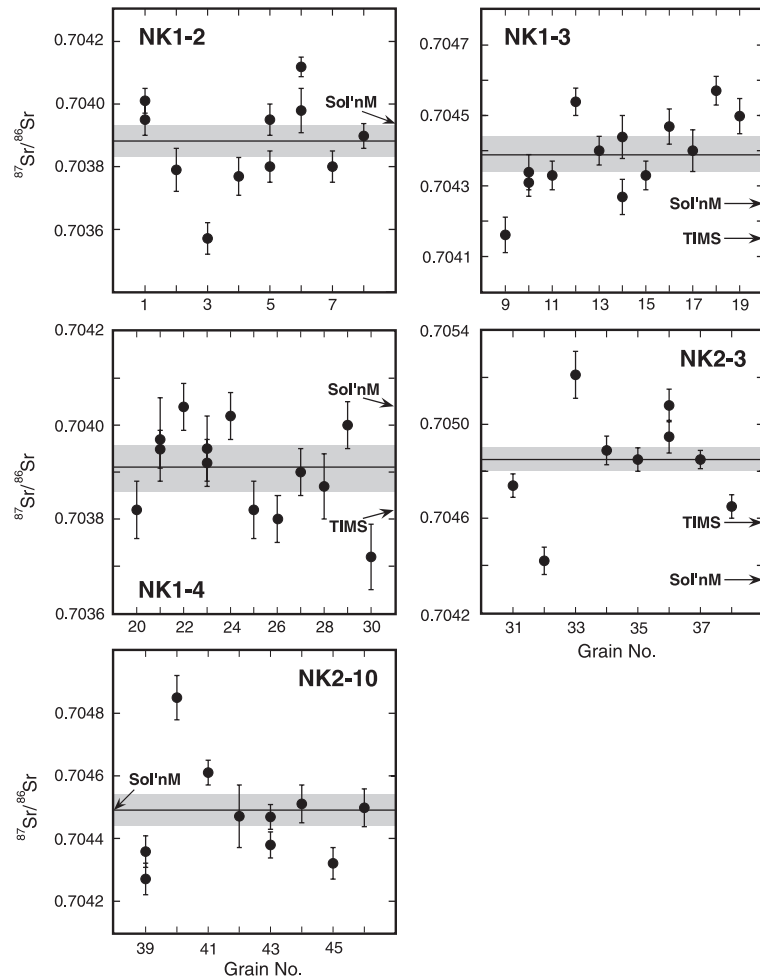


Fig. 3. Individual  $^{87}\text{Sr}/^{86}\text{Sr}$  isotope analyses of clinopyroxenes for five garnet peridotites from the Nikos kimberlite. Horizontal line across diagram represents average value for laser ablation analyses. Sol'nM =  $^{87}\text{Sr}/^{86}\text{Sr}$  value obtained by solution mode MC-ICP-MS; TIMS =  $^{87}\text{Sr}/^{86}\text{Sr}$  value obtained by thermal ionization mass spectrometry. Shaded array outlines external reproducibility (0.00005;  $2\sigma$ ). Error bars represent internal precisions of individual laser ablation analyses at the  $2\sigma$  level.

both solution mode MC-ICP-MS and TIMS represent a weighted average value of the Sr isotopic composition for the clinopyroxene separates. The relatively large difference between the  $^{87}\text{Sr}/^{86}\text{Sr}$  compositions obtained by solution mode MC-ICP-MS and TIMS for three samples (Table 1, Fig. 3) may be attributed to the different number of grains (50 versus 150, respectively) used in each method, and/or the fact that the two clinopyroxene separates were obtained from different portions of the xenolith sample (size  $\sim 10$  cm). The differences between solution mode MC-ICP-MS versus TIMS results suggest isotopic heterogeneities on

the scale of a single xenolith ( $>10$  cm), and support the existence of Sr isotopic variation obtained by the laser ablation analyses for individual clinopyroxenes.

At least one grain was ablated twice in each sample (for a total of 10 pairs) in order to evaluate the degree of isotopic homogeneity within single grains. For most grains, the Sr isotopic values obtained for the two analyses are identical (within error), or just outside their associated analytical uncertainties by 0.2‰ (i.e. variation of  $\sim 0.00015$ ; e.g. grain nos. 5-1 and 5-2; nos. 6-1 and 6-2 from NK1-2; Table 1). These results suggest that individual clinopyroxene grains in the

Nikos peridotites mainly exhibit internal Sr isotopic equilibrium, despite the differences observed between grains.

Mineral compositions were obtained by electron microprobe analysis for clinopyroxene grains analyzed by laser ablation in order to investigate possible metasomatic effects on their major element abundances (Table 3). The SiO<sub>2</sub> contents in the clinopyroxenes correlate negatively and TiO<sub>2</sub> abundances correlate positively with their respective Sr isotopic ratios, and trend towards the composition of the Nikos kimberlite (Tables 1 and 3; Fig. 4a and b). Contrarily, CaO, MgO, FeO and Al<sub>2</sub>O<sub>3</sub> abundances in the clinopyroxenes (not shown) do not correlate with Sr isotopic values (Tables 1 and 3). One possible explanation is that these elements occur at similar concentration levels in both clinopyroxene and kimberlite (Schmidberger and Francis, 2001).

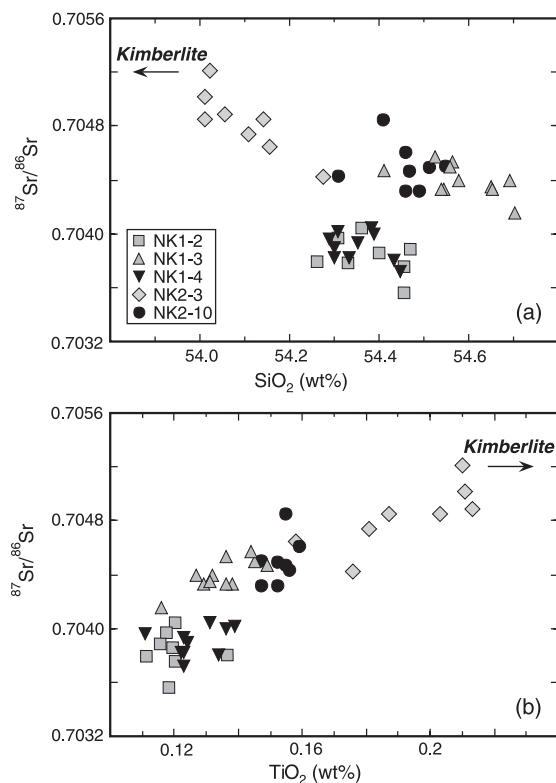


Fig. 4. Plot of  $^{87}\text{Sr}/^{86}\text{Sr}$  isotope ratios obtained by laser ablation MC-ICP-MS versus (a) SiO<sub>2</sub> and (b) TiO<sub>2</sub> contents for individual clinopyroxene grains from Nikos peridotites.

#### 4. Discussion

Experimental data on Sr diffusion in diopside have shown that isotopic equilibration at the mineral (mm) scale should occur over time periods of 1 to 100 Ma at lithospheric temperatures of 900 to 1000 °C (Sneeringer et al., 1984). This is in agreement with previous findings based on diffusion data in mantle minerals, which indicate that isotopic disequilibrium between mineral phases cannot be maintained at 1000 °C for more than a few million years (Hofmann and Hart, 1978). The experimental results also indicate that the presence of a melt will reduce the time required to achieve isotopic equilibrium (<0.1 Ma). Previous studies of mantle xenoliths are consistent with these experimental results, and suggest that isotopic disequilibrium between constituent peridotite minerals (e.g. clinopyroxene and garnet) can only be preserved in the shallow lithospheric mantle at temperatures below 900 °C (Macdougall and Haggerty, 1999). The deeper lithospheric mantle should thus be at sufficiently high temperatures to eliminate isotopic disequilibria rapidly. It has also been demonstrated that  $^{143}\text{Nd}/^{144}\text{Nd}$  isotopic equilibrium may be achieved in clinopyroxene in ~ 1 Ma at near solidus conditions of peridotite (i.e. ~ 1450 °C; 25 kb; Van Orman et al., 2001). The time for isotopic equilibration in the lithosphere, however, may increase to ~ 1000 Ma at the lower eclogite solidus temperatures (i.e. 1150 °C at 15 kb; Van Orman et al., 2001). Despite these experimental results, isotopic heterogeneity has been documented in melt inclusions in olivine crystals from oceanic basalts by in situ analysis, which records small-scale Pb isotopic disequilibrium between different inclusions within single olivine crystals (Saal et al., 1998; Shimizu et al., 1999).

The laser ablation Sr isotopic ratios of clinopyroxene grains from the Nikos peridotites show a significant compositional range within individual xenoliths, and establish the existence of  $^{87}\text{Sr}/^{86}\text{Sr}$  heterogeneities between grains (Table 1; Fig. 3). The  $^{87}\text{Sr}/^{86}\text{Sr}$  ratios do not correlate with  $^{85}\text{Rb}$  intensities, which indicates that the observed variations are not the result of long-term radiogenic ingrowth. These findings indicate that small-scale (mm) Sr isotopic heterogeneities exist in the lithospheric mantle that last equilibrated at temperatures of at least 1100 °C and depths of 150 km. This interpretation is supported by the relatively large

difference in the  $^{87}\text{Sr}/^{86}\text{Sr}$  compositions obtained by solution mode MC-ICP-MS and TIMS for clinopyroxene separates from different portions of individual xenoliths (Fig. 3). Clinopyroxenes from kimberlite-hosted peridotites commonly exhibit a large variation in Sr values (determined by TIMS), and the range in Sr isotopic ratios ( $^{87}\text{Sr}/^{86}\text{Sr}_{(t)} = 0.70357\text{--}0.70521$ ; Table 1) obtained here for the Nikos clinopyroxenes is similar to that reported for clinopyroxenes in peridotite xenoliths from single kimberlite pipes (e.g. Kimberley, Bultfontein, Jagersfontein) from the South African Kaapvaal craton (e.g. Menzies and Murthy, 1980; Kramers et al., 1983; Walker et al., 1989).

The whole rock Nd, Pb and Sr isotope systematics for the Nikos peridotites (Schmidberger et al., 2001) suggests that these xenoliths have probably suffered a small amount ( $\sim 1$  wt.%) of kimberlite contamination during sample transport. The Sr isotopic variability in clinopyroxene recorded by the laser ablation data could thus be attributed to interaction with the host kimberlite magma. The presence of fine-grained and possibly kimberlite-related inclusions in clinopyroxene characterized by high  $^{87}\text{Rb}/^{86}\text{Sr}$  ratios (e.g. phlogopite), however, cannot account for the observed Sr isotopic variation within individual samples because only inclusion-free grains were used for the ablation experiments. These findings are supported by high internal precisions for individual laser analyses (Table 1), which would not be obtained if mineral inclusions (with different isotopic compositions) were present.

The clinopyroxenes showing the least radiogenic  $^{87}\text{Sr}/^{86}\text{Sr}$  values (0.7036, NK1-2, grain no. 3; 0.7037, NK1-4, grain no. 30; Table 1) could be interpreted to represent the best estimate of 'uncontaminated' depleted subcontinental mantle. In comparison, the Nikos kimberlite (average of five samples) is characterized by a significantly more radiogenic whole rock  $^{87}\text{Sr}/^{86}\text{Sr}$  composition of 0.7052 at the time of emplacement (i.e. 100 Ma ago; Schmidberger et al., 2001). The addition of this kimberlite component would result in an increase of the  $^{87}\text{Sr}/^{86}\text{Sr}$  ratios in the Nikos clinopyroxenes, since the kimberlite is characterized by much higher Sr contents (1000–2200 ppm) than the clinopyroxenes (100–400 ppm; Schmidberger and Francis, 2001). Thus, the highest Sr isotopic values would be recorded by clinopyroxenes

that had experienced the largest degree of metasomatic interaction with the host kimberlite.

The trends between  $\text{SiO}_2$  and  $\text{TiO}_2$  contents for the clinopyroxenes versus their respective Sr isotope compositions (Tables 1 and 3; Fig. 4a and b) are unlikely to reflect depth-dependent partitioning since the abundances of these two major elements do not correlate with estimated temperatures or pressures of last equilibration in the mantle (Schmidberger and Francis, 1999). There are large differences in the concentration levels of  $\text{SiO}_2$  and  $\text{TiO}_2$  between clinopyroxenes ( $\text{SiO}_2 \sim 54$  wt.%;  $\text{TiO}_2 \sim 0.14$  wt.%) and kimberlite ( $\text{SiO}_2 \sim 23$  wt.%;  $\text{TiO}_2 \sim 1.8$  wt.%), and their correlations with Sr isotopic ratios imply that kimberlite metasomatism has also affected the chemical compositions of the clinopyroxenes. These findings are in good agreement with previously determined light rare earth element (LREE) abundances for three of the samples investigated in this study (e.g. Ce: NK1-4 = 20 ppm, NK1-3 = 30 ppm, NK2-3 = 50 ppm; Schmidberger and Francis, 2001), which correlate positively with their respective  $^{87}\text{Sr}/^{86}\text{Sr}$  ratio (NK1-4 = 0.7039, NK1-3 = 0.7044, NK2-3 = 0.7048).

In addition to their overall shift towards the kimberlite composition, the samples that are characterized by higher average  $^{87}\text{Sr}/^{86}\text{Sr} > 0.7044$  (NK1-3, NK2-10, NK2-3) also exhibit intra-sample compositional variations that trend toward that of the host magma (Fig. 4a and b). Of interest, sample NK2-3 plots closest to the compositional field for the Nikos kimberlite and exhibits the largest intra-sample variation in  $^{87}\text{Sr}/^{86}\text{Sr}$  ratios (1.1‰; Figs. 3 and 4). These clinopyroxenes also yield a large difference (outside the external reproducibility) between the average  $^{87}\text{Sr}/^{86}\text{Sr}$  value calculated for individual laser ablation runs and the corresponding value obtained either by solution mode MC-ICP-MS or TIMS. In contrast, clinopyroxenes from samples NK1-2 and NK1-4 are interpreted to represent the best estimate of 'uncontaminated' depleted subcontinental mantle since these are characterized by the lowest average  $^{87}\text{Sr}/^{86}\text{Sr}$  ratios (0.7039), and show little trend towards the kimberlite compositional field (Fig. 4a and b).

The rather large degree of intra- and inter-sample Sr isotopic heterogeneity recorded by the clinopyroxenes in the Nikos peridotites appears to reflect metasomatic activity associated with kimberlite magmatism 100 Ma ago. The Sr isotopic variations, and their

correlation with SiO<sub>2</sub>, TiO<sub>2</sub> and LREE abundances, suggest an increasing amount of interaction between clinopyroxenes and the host kimberlite from samples NK1-4 and NK1-2 (low) to NK1-3 and NK2-10 (intermediate) to NK2-3 (high). The existing experimental data on the diffusion of Sr at mantle temperatures and pressures near the peridotite solidus suggest that metasomatic activity could not precede sample entrainment by more than ~ 1 Ma. Thus, the preservation of the Sr isotope variability suggests that metasomatism would have occurred during kimberlite magmatism, either just prior to or during kimberlite transport. The preservation of these Sr isotopic heterogeneities indicates that closure temperatures for Sr diffusion in clinopyroxenes were attained rapidly after emplacement in the continental crust.

## 5. Conclusions

This study is the first to report in situ <sup>87</sup>Sr/<sup>86</sup>Sr analyses of individual clinopyroxene grains from peridotite xenoliths. The results demonstrate the ability of a laser ablation MC-ICP-MS system to perform in situ isotope analyses on mantle phases. The Sr isotopic results document large variations in clinopyroxene separates from different samples, and between clinopyroxene grains within individual xenolith samples, which amount to as much as 1.1‰ (8 parts in 7000). The Sr isotopic ratios obtained for the clinopyroxene separates correlate with abundances of SiO<sub>2</sub> and TiO<sub>2</sub>, which is consistent with the introduction of a kimberlite component in the clinopyroxenes. It thus appears likely that the large degree of intra-sample isotopic heterogeneity is the result of metasomatic activity associated with kimberlite magmatism. The preservation of Sr isotope variability suggests that metasomatism probably occurred just prior to or during kimberlite transport, since Sr diffusion would eradicate existing isotope heterogeneities at time scales of ~ 1 Ma at mantle temperatures and pressures.

The findings of this study suggest that isotopic compositions obtained on bulk mineral separates from peridotite xenoliths likely represent weighted averages of heterogeneous populations. This heterogeneity might in large part reflect interaction with their host magma and complicates the interpretation of isotopic

differences between samples. The implications of isotopic studies using mineral separates may thus need to be reexamined by in situ techniques.

## Acknowledgements

We thank Joel Visser (Merchantek-New Wave Research) for providing the ablation cell and for technical support. The MC-ICP-MS laboratory at GEOTOP is maintained in part with an NSERC MFA grant, and the research was funded by an NSERC operating grant to D. Francis. S. Schmidberger is grateful for financial support in the form of an NSERC doctoral scholarship. [RR]

## References

- Allègre, C.J., Hamelin, B., Provost, A., Dupré, B., 1986. Topology in isotopic multispace and origin of mantle chemical heterogeneities. *Earth Planet. Sci. Lett.* 81, 319–337.
- Bizzarro, M., Simonetti, A., Stevenson, R.K., Kurszlaukis, S., 2003. In situ <sup>87</sup>Sr/<sup>86</sup>Sr investigation of igneous apatites and carbonates using laser-ablation MC-ICP-MS. *Geochim. Cosmochim. Acta* 67, 289–302.
- Christensen, J.N., Halliday, A.N., Der-Chuen, L., Hall, C.M., 1995. In situ Sr isotopic analysis by laser ablation. *Earth Planet. Sci. Lett.* 136, 79–85.
- Davidson, J., Tepley III, F., Palacz, Z., Meffan-Main, S., 2001. Magma recharge, contamination and residence times revealed by in situ laser ablation isotopic analysis of feldspar in volcanic rocks. *Earth Planet. Sci. Lett.* 184, 427–442.
- Eggs, S.M., Kinsley, L.P.J., Shelley, J.M.G., 1998. Deposition and element fractionation processes during atmospheric pressure sampling for analysis by ICP-MS. *Appl. Surf. Sci.* 127–129, 278–286.
- Faure, G., 1986. *Principles of Isotope Geology*. Wiley, New York, p. 589.
- Frisch, T., Hunt, P.A., 1993. Reconnaissance U–Pb geochronology of the crystalline core of the Boothia Uplift, District of Franklin, Northwest Territories. *Radiogenic Age and Isotope Studies: Report 7*. *Geol. Surv. Canada Paper* 93-2, 3–22.
- Hart, S.R., Hauri, E.H., Oschmann, L.A., Whitehead, J.A., 1992. Mantle plumes and entrainment: isotopic evidence. *Science* 256, 517–520.
- Hawkesworth, C.J., Erlank, A.J., Kempton, P.D., Waters, F.G., 1990. Mantle metasomatism: Isotope and trace-element trends in xenoliths from Kimberley, South Africa. *Chem. Geol.* 85, 19–34.
- Heaman, L.H., 1989. The nature of the subcontinental mantle from Sr–Nd–Pb isotopic studies on kimberlite perovskite. *Earth Planet. Sci. Lett.* 92, 323–334.

- Hofmann, A.W., 1997. Mantle geochemistry: the message from oceanic volcanism. *Nature* 385, 219–229.
- Hofmann, A.W., Hart, S.R., 1978. An assessment of local and regional isotopic equilibrium in the mantle. *Earth Planet. Sci. Lett.* 38, 44–62.
- Horn, I., Rudnick, R.L., McDonough, W.F., 2000. Precise elemental and isotope ratio determination by simultaneous solution nebulization and laser ablation-ICP-MS: application to U–Pb geochronology. *Chem. Geol.* 164, 281–301.
- Jackson, S.E., Pearson, N.J., Griffin, W.L., 2001. In situ isotope ratio determination using laser-ablation (LA)–magnetic sector-ICP-MS. In: Sylvester, P.J. (Ed.), *Laser-Ablation-ICP-MS in the Earth Sciences. Short course series-Mineral. Assoc. Canada*, vol. 29, pp. 105–119.
- Kinny, P.D., Dawson, J.B., 1992. A mantle metasomatic injection event linked to late Cretaceous kimberlite magmatism. *Nature* 360, 726–728.
- Kramers, J.D., Roddick, J.C.M., Dawson, J.B., 1983. Trace element and isotope studies on veined, metasomatic and MARID xenoliths from Bultfontein, South Africa. *Earth Planet. Sci. Lett.* 65, 90–106.
- Macdougall, J.D., Haggerty, S.E., 1999. Ultradeep xenoliths from African kimberlites: Sr and Nd isotopic compositions suggest complex history. *Earth Planet. Sci. Lett.* 170, 73–82.
- Mason, P., 2001. Expanding the capabilities of laser-ablation ICP-MS with collision and reaction cells. In: Sylvester, P.J. (Ed.), *Laser-Ablation-ICP-MS in the Earth Sciences. Short course series-Mineral. Assoc. Canada*, vol. 29, pp. 63–82.
- McDonough, W.F., McCulloch, M.T., 1987. The southeast Australian lithospheric mantle: implications for its growth and evolution. *Earth Planet. Sci. Lett.* 86, 327–340.
- McDonough, W.F., Sun, S.S., 1995. The composition of the Earth. *Chem. Geol.* 120, 223–253.
- Menzies, M.A., Murthy, R., 1980. Enriched mantle: Nd and Sr isotopes in diopsides from kimberlite nodules. *Nature* 283, 634–636.
- Pell, J., 1993. New kimberlite discoveries on Somerset Island. *Exploration Review* 1993. NWT Geology Division, Department of Indian and Northern Affairs, Yellowknife, p. 47.
- Rudnick, R.L., McDonough, W.F., Chappell, B.W., 1993. Carbonatite metasomatism in the northern Tanzanian mantle. *Earth Planet. Sci. Lett.* 114, 463–475.
- Russell, W.A., Papanastassiou, D.A., Tombrello, T.A., 1978. Ca isotope fractionation on the Earth and other solar system materials. *Geochim. Cosmochim. Acta* 42, 1075–1090.
- Saal, A.E., Hart, S.R., Shimizu, N., Hauri, E.H., Layne, G.D., 1998. Pb isotopic variability in melt inclusions from oceanic island basalts, Polynesia. *Science* 282, 1481–1484.
- Schmidberger, S.S., Francis, D., 1999. Nature of the mantle roots beneath the North American craton: mantle xenolith evidence from Somerset Island kimberlites. *Lithos* 48, 195–216.
- Schmidberger, S.S., Francis, D., 2001. Constraints on the trace element composition of the Archean mantle root beneath Somerset Island, Arctic Canada. *J. Petrol.* 42, 1095–1117.
- Schmidberger, S.S., Simonetti, A., Francis, D., 2001. Sr–Nd–Pb isotope systematics of mantle xenoliths from Somerset Island kimberlites: evidence for lithosphere stratification beneath Arctic Canada. *Geochim. Cosmochim. Acta* 65, 4243–4255.
- Shimizu, N., Sobolev, A.V., Layne, G.D., Tsamirian, O.P., 1999. Large lead-isotopic variations in olivine-hosted melt inclusions in a basalt from the mid-Atlantic ridge. Ninth Annual V.M. Goldschmidt Conference LPI Contribution No. 971. Lunar and Planetary Institute, Houston, p. 273.
- Simonetti, A., Bell, K., 1993. Isotopic disequilibrium in clinopyroxenes from nephelinitic lavas, Napak volcano, eastern Uganda. *Geology* 21, 243–246.
- Smith, C.B., Allsopp, H.L., Garvie, O.G., Kramers, J.D., Jackson, P.F.S., Clement, C.R., 1989. Note on the perovskite method for dating kimberlites: examples from the Wesselton and DeBeers mines, South Africa, and Somerset Island, Canada. *Chem. Geol.* 79, 137–145.
- Sneeringer, M., Hart, S.R., Shimizu, N., 1984. Strontium and samarium diffusion in diopside. *Geochim. Cosmochim. Acta* 48, 1589–1608.
- Van Orman, J.A., Grove, T.L., Shimizu, N., 2001. Rare earth element diffusion in diopside: influence of temperature, pressure, and ionic radius, and an elastic model for diffusion in silicates. *Contrib. Mineral. Petrol.* 141, 687–703.
- Walker, R.J., Carlson, R.W., Shirey, S.B., 1989. Os, Sr, Nd, and Pb isotope systematics of southern African peridotite xenoliths: implications for the chemical evolution of subcontinental mantle. *Geochim. Cosmochim. Acta* 53, 1583–1595.
- Yaxley, G.M., Crawford, A.J., Green, D.H., 1991. Evidence for carbonatite metasomatism in spinel peridotite xenoliths from western Victoria. *Earth Planet. Sci. Lett.* 107, 305–317.
- Zhang, H.-F., Matthey, D.P., Grassineau, N., Lowry, D., Brownless, M., Gurney, J.J., Menzies, M.A., 2000. Recent fluid processes in the Kaapvaal Craton, South Africa: coupled oxygen isotope and trace element disequilibrium in polymict peridotites. *Earth Planet. Sci. Lett.* 176, 57–72.
- Zindler, A., Hart, S.R., 1986. Chemical geodynamics. *Annu. Rev. Earth Planet. Sci.* 14, 493–571.